ELSEVIER

Experimental and theoretical investigations of ionization potentials and structures of mixed sodium lithium clusters

E. Benichou, A.R. Allouche, M. Aubert-Frecon, R. Antoine, M. Broyer,
Ph. Dugourd [*], D. Rayane

Laboratoire de Spectrométrie Ionique et Moléculaire (UMR n°5579), CNRS et Université, Lyon I, bât. 205, 43 Bd du 11 Novembre 1918, 69622 Villeurbanne Cedex, France

Abstract

We have measured the ionization potentials (IP) of $Na_{n-m}Li_m$ clusters ($3 \leq n \leq 21$ and $1 \leq m \leq 3$) generated in a supersonic beam. The IPs of mixed clusters are close to the values obtained for pure sodium and pure lithium clusters. They display the features of a metallic system with n delocalized electrons. For clusters containing 2–6 atoms, we have performed density functional theory calculations. The IPs calculated for the lowest-energy structures are in good agreement with experiment. The geometries of the heteronuclear clusters, in particular the 2D–3D transition, are discussed in detail. © 1998 Elsevier Science B.V. All rights reserved.

1. Introduction

Pure alkali clusters are considered as models for metallic clusters. They have been extensively studied. In particular, the comparison of optical spectra and CI ab initio calculations have allowed a precise determination of the geometries and of the electronic properties of small lithium and sodium clusters [1–5]. While lithium and sodium atoms have the same external electronic structure and both solids are perfect metals with similar crystal structure, lithium and sodium clusters present significant differences. The most striking differences have been observed for the optical absorption spectra. Both small sodium and small lithium clusters display a strong absorption in

the blue. In sodium clusters, this resonance is reasonably described in the frame of a simple Mie–Drude model with fully delocalized valence electrons [6,7]. The resonances calculated with this model for lithium clusters are strongly shifted toward high energies as compared to experimental spectra [1]. This shift can be corrected by introducing an effective mass for the valence electrons and is mainly due to the fact that the electronic inner shell of the lithium atom contains only s-electrons while the inner shell of sodium atom also contains p-electrons (1s, 2s and 2p shells). Due to this difference in electronic structure, the valence electron–ion interactions are reasonably described by local potentials in sodium clusters, but it is necessary to take into account the non-local nature of these interactions in lithium clusters [8]. The importance of the non-locality to interpret the electronic properties of lithium clusters has recently been

---

[*] Corresponding author.
E-mail: dugourd@hplasim2.univ-lyon1.fr

confirmed by dipole polarizability measurements [9]. Geometrical differences have also been observed between small sodium and small lithium clusters. The most visual difference is the fact that the 2D–3D transition does not occur for the same size. It occurs between 6 and 7 in sodium clusters, while it occurs between 4 and 5 or 5 and 6 in lithium clusters [2,10].

Finally, as far as ionization potentials (IP) are concerned, it seems that the sodium clusters IPs change regularly from the atom to the bulk, as expected for a finite metallic sphere, while the size evolution for lithium is not as simple [11]. The comparison of the IPs of sodium and lithium clusters, which we have measured with similar conditions, shows that the lithium values cross the sodium values at around a size of 8. A second crossing has to occur before the bulk limit. The size range of this second crossing has not yet been determined. In fact, the lithium IPs measured on small sizes are well reproduced by ab initio calculations [12] and some recent Jellium-related models [13], but the size evolution is puzzling.

It appears that despite the numerous experimental and theoretical works on alkali clusters, the particularities of sodium and lithium clusters are not yet fully understood. In particular the connection between electronic and geometrical differences, which is one of the most open questions in solid or cluster science, is not clear even for these simple systems. The study of mixed lithium sodium clusters gives new insights into these differences. Up to date, the only available experimental results were abundances in mass spectra [14] and optical spectra for tetramers [15]. In this Letter we present the measurement of IPs of mixed lithium sodium clusters. Experimental results obtained for small sizes are compared with density functional theory calculations (DFT). The 2D–3D transition being one of the most important steps towards the bulk, we focus our discussion on the geometrical differences observed for small sizes.

2. Experiment

Alkali clusters are produced in a supersonic molecular beam. Briefly, the metal is heated in a TZM cartridge at 1100 K. A mixture of metal vapor and of 3 bars of argon expands through a 100 μm diameter nozzle. The collinear part of the beam is extracted by a skimmer. In order to produce mixed clusters, isotopically purified lithium (^{7}Li) and sodium metals are put in the cartridge. The vapor pressure of Na and Li, at 1100 K, are 400 and 6 Torr, respectively. Clusters are ionized 30 cm after the source by an XeCl pumped tunable dye laser. The ionization laser was scanned from 260 to 350 nm. Wavelengths inferior to 330 nm were obtained by frequency doubling in BBO and KDP crystals. The laser power was maintained around 100 μJ/cm^2. We carefully checked that no multiphotonic effect took place for this power. After ionization, clusters are mass selected in a time-of-flight mass spectrometer and detected on microchannel plates. The signal is averaged with a 100 MHz numerical oscilloscope and recorded on a personal computer.

With the source conditions described above, Na_nLi_m clusters with $n = 1$–21 and $m = 0$–3 were observed. Photoionization cross-sections were obtained for each mass by systematically recording mass spectra every 2 nm. IPs are determined by linear extrapolation. Pure lithium clusters IPs were determined in a previous experiment with only lithium metal in the oven [16]. Photoionization cross-sections and IPs of pure sodium clusters are identical to the values that we have recently reported in Ref. [17]. Comparison with previous values in the literature are discussed in this reference. A precise experimental determination of absolute IPs is difficult, it depends on the way one extrapolates the photoionization cross-sections and on the source conditions. In particular, the IPs measured for cold sodium clusters produced with a laser vaporization source are slightly different from our values [11,18]. Thus, in this Letter, we compare experimental IPs of mixed clusters to the IPs that we have measured for pure alkali clusters with the same source and the same method of extrapolation.

3. Calculations

Non-local spin density calculations (all-electron) were performed with the Perdew–Wang-91 gradient-corrected functional [19] using the package GAUSSIAN 94 [20]. Gaussian basis sets 6-31G were used both for lithium and sodium atoms. First, the

lowest-energy geometry has been determined for each neutral $Na_{n-m}Li_m$ and ionic $Na_{n-m}Li_m^+$ cluster for $n + m = 2$–6. Geometry optimizations were performed via gradient methods, using as initial configurations those obtained from previous ab initio calculations for pure neutral M_n and cationic M_n^+ alkali clusters [4,5,12,21,22]. Then adiabatic and vertical ionization potentials have been obtained for the lowest-energy geometries so obtained.

4. Experimental results

The ionization potentials that we have measured are given in Table 1 and shown in Fig. 1. For heterogeneous clusters with 11 atoms, the signal was small and we were not able to obtain precise IPs. They are not reported in the table. IPs of sodium and lithium clusters are of the same order of magnitude and are characterized by similar odd–even alternations and shell effects. The IP of the Li atom (5.39 eV) and the workfunction of the Li metal (2.9 eV) are higher than the values for sodium (5.14 and 2.75 eV, respectively) [23]. As expected IPs of small
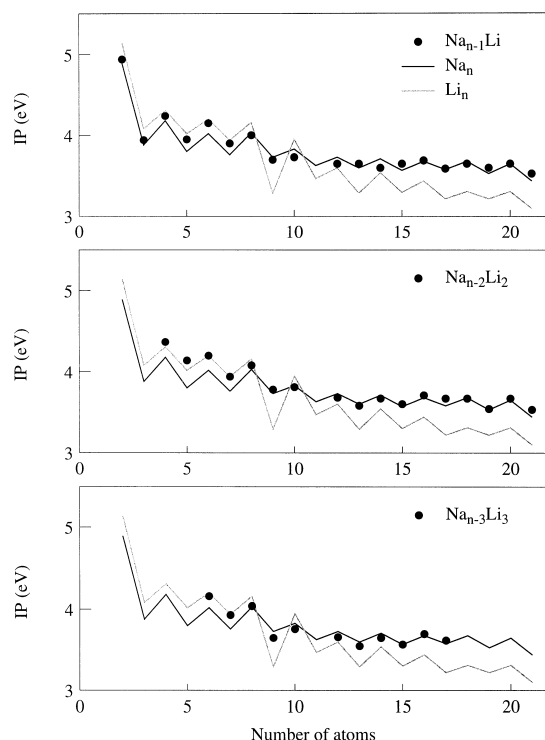

Fig. 1. Ionization potentials of $Na_{n-1}Li$, $Na_{n-2}Li_2$ and $Na_{n-3}Li_3$ clusters plotted as a function of the number of atoms in the cluster (black circles). These values are compared to the values measured for pure sodium clusters (black line) and pure lithium clusters (gray line).

Table 1
Experimental ionization potentials of Na_nLi_m clusters

n	IP (eV)				
	Na_n	$Na_{n-1}Li$	$Na_{n-2}Li_2$	$Na_{n-3}Li_3$	Li_n
3	3.88	3.94			4.08
4	4.18	4.24	4.37		4.31
5	3.80	3.95	4.14		4.02
6	4.02	4.15	4.20	4.16	4.20
7	3.76	3.90	3.94	3.93	3.94
8	4.03	4.00	4.08	4.04	4.16
9	3.73	3.70	3.78	3.65	3.29
10	3.83	3.73	3.81	3.76	3.95
11	3.63				3.47
12	3.73	3.65	3.68	3.66	3.60
13	3.60	3.65	3.58	3.55	3.29
14	3.71	3.60	3.67	3.65	3.54
15	3.57	3.65	3.60	3.57	3.30
16	3.68	3.69	3.71	3.70	3.44
17	3.58	3.59	3.67	3.62	3.22
18	3.68	3.65	3.67		3.31
19	3.53	3.60	3.54		3.22
20	3.65	3.65	3.67		3.31
21	3.44	3.53	3.53		3.10

The uncertainty is in the range of 0.1 eV.

lithium clusters are greater than IPs of small sodium clusters. However, for every size greater than 10 which we have studied, the IPs of lithium clusters are smaller than the IPs of the sodium clusters. As mentioned in Section 1, this anomaly is not fully understood. IPs of mixed clusters are roughly distributed between the values of pure sodium and pure lithium clusters. The odd–even alternation and the shell effects observed for Na_nLi_m clusters are similar to those observed for pure alkali clusters, they are characteristic of a metallic cluster with $n + m$ delocalized electrons. This is not surprising and was already observed for small Na_nK_m clusters [24] and NaK_n clusters [25]. For clusters with more than 8 atoms, the IPs of the mixed clusters that we have observed are close to the IPs of pure sodium clusters. In particular, the amplitude of the shell effect observed between 8 and 9 electrons (completion of the

1p shell) is similar to the amplitude observed for sodium clusters. This result is not surprising, because all the large clusters that we have studied are rich in sodium. In the following sections we focus our discussion on small sizes for which we observed clusters with different concentrations of lithium.

5. Comparison with calculated values and discussion

Experimental results are compared with results of our DFT/PW-91 calculations for sizes from 2 to 6. Calculated results for the energy, symmetry, adiabatic and vertical ionization potentials of the lowest-

energy structure that we have obtained for Na_nLi_m clusters with $2 \leqslant n + m \leqslant 6$ are given in Table 2. IPs obtained for pure sodium and lithium clusters and mixed trimers are compared to experimental values and to CI ab initio calculations [26,21,27]. The calculated energy and the symmetry of the lowest-energy structures obtained for $Na_nLi_m^+$ cationic clusters are given in Table 3.

5.1. Dimers

The calculated IPs for homonuclear and heteronuclear dimers are in good agreement with experimental values. Experimental values are $IP(Na_2) = 4.89$ eV [28], $IP(NaLi) = 4.94$ eV [29], $IP(Li_2) = 5.14$ eV

Table 2
Ground-state energies and properties of optimized neutral Na_nLi_m clusters

Cluster		Symm	State	Energy (au)	$E_b/(n+m)$ [a] (eV)	IPa/IPv [b] (eV)	IPa/IPv (CI) [c] (eV)	IPa/IPv (CI) [d] (eV)	IP Exp (eV)
Na_2		$D_{\infty h}$	$^1\Sigma_g^+$	-324.54737	0.30	4.88/4.98	4.47/4.60	4.89/5.02	4.89[e]
$NaLi$		$C_{\infty v}$	$^1\Sigma^+$	-169.77091	0.33	4.98/5.07		4.99/5.18	4.94[f]
Li_2		$D_{\infty h}$	$^1\Sigma_g^+$	-14.99471	0.37	5.07/5.15	5.01/5.07	5.21/5.36	5.14[g]
Na_3	(obtuse)	C_{2v}	$^2B_2$	-486.82092	0.29	4.02/4.20	3.69/3.76	3.87/4.05	3.88
Na_2Li	(obtuse)	C_{2v}	$^2B_2$	-332.04811	0.35	4.11/4.26		3.96/4.05	3.94
$NaLi_2$		C_s	$^2A'$	-177.27366	0.39	4.17/4.25		4.03/4.22	
Li_3	(obtuse)	C_{2v}	$^2B_2$	-22.49962	0.44	4.21/4.30	4.03/4.14	4.10/4.20	4.08
Na_4	(rhombus)	D_{2h}	^1A_g	-649.10730	0.38	4.16/4.17	3.90/3.97		4.18
Na_3Li	(rhombus)	C_{2v}	$^1A_1$	-494.33758	0.44	4.24/4.25			4.24
Na_2Li_2	(rhombus)	D_{2h}	^1A_g	-339.56831	0.51	4.33/4.35			4.37
$NaLi_3$	(rhombus)	C_{2v}	$^1A_1$	-184.79348	0.54	4.37/4.39			
Li_4	(rhombus)	D_{2h}	^1A_g	-30.01870	0.57	4.42/4.44	4.56/4.57		4.31
Na_5	(planar)	C_{2v}	$^2A_1$	-811.39283	0.43	3.93/4.19	3.63/3.88		3.80
Na_4Li	(planar)	C_{2v}	$^2A_1$	-656.62470	0.49	4.00/4.20			3.95
Na_3Li_2	(planar)	C_s	$^2A^+$	-501.85333	0.53	4.11/4.27			4.14
Na_2Li_3	(planar)	C_{2v}	$^2A_1$	-347.08241	0.57	4.12/4.35			
$NaLi_4$	(bipyr.)	C_s	$^2A'$	-192.30886	0.60	4.14/4.25			
Li_5	(bipyr.)	C_{2v}	$^2B_1$	-37.53601	0.64	4.18/4.28	3.98/4.05		4.02
Na_6	(pyr. Pent.)	C_{5v}	$^1A_1$	-973.68474	0.49	4.12/4.38	3.83/3.99		4.02
Na_5Li	(plan Pent.)	D_{5h}	$^1A_1'$	-818.92257	0.57	4.22/4.42			4.15
Na_4Li_2	(bipyr.)	D_{4h}	$^1A_{1g}$	-664.15176	0.60	4.13/4.33			4.2
Na_3Li_3	(bipyr.)	C_{2v}	$^1A_1$	-509.37982	0.63	4.13/4.36			4.16
Na_2Li_4	(bipyr.)	C_{2v}	$^1A_1$	-354.60812	0.67	4.12/4.30			
$NaLi_5$	(bipyr.)	C_{2v}	$^1A_1$	-199.83516	0.70	4.15/4.45			
Li_6	(bipyr.)	D_{4h}	$^1A_1$	-45.06233	0.72	4.18/4.49	4.14/4.27		4.2

[a] Binding energy per atom $E_b/(n+m)$ for Na_nLi_m: $[nE(Na) + mE(Li) - E(Na_nLi_m)]/(n+m)$.
[b] Present results.
[c] Theoretical values from Ref. [26] for pure lithium clusters and Ref. [21] for pure sodium clusters.
[d] Theoretical values from Ref. [27].
[e] Experimental values from Ref. [28].
[f] Experimental values from Ref. [29].
[g] Experimental values from Ref. [30].

Table 3
Symmetry and ground-state energy of optimized cationic $Na_nLi_m^+$ clusters

Cluster		Symm.	Energy (au)	$E_b + /n$ [a] (eV)
Na_2^+		$D_{\infty h}$	−324.36791	0.48
$NaLi^+$		$C_{\infty v}$	−169.58800	0.47
Li_2^+		$D_{\infty h}$	−14.80828	0.60
Na_3^+	(equilateral)	D_{3h}	−486.67309	0.70
Na_2Li^+	(obtuse)	C_{2v}	−331.89691	0.73
$NaLi_2^+$	(acute)	C_{2v}	−177.12036	0.75
Li_3^+	(equilateral)	D_{3h}	−22.34462	0.88
Na_4^+	(rhombus)	D_{2h}	−648.9545	0.65
Na_3Li^+	(rhombus)	C_{2v}	−494.1819	0.70
$Na_2Li_2^+$	(rhombus)	D_{2h}	−339.40923	0.74
$NaLi_3^+$	(rhombus)	C_{2v}	−184.63285	0.76
Li_4^+	(rhombus)	D_{2h}	−29.85613	0.85
Na_5^+	(2 triangles 3D)	D_{2d}	−811.24826	0.69
Na_4Li^+	(2 triangles 3D)	D_{2d}	−656.47760	0.74
$Na_3Li_2^+$	(2 triangles 3D)	/	−501.70225	0.76
$Na_2Li_3^+$	(bipyramid)	D_{3h}	−346.93114	0.80
$NaLi_4^+$	(bipyramid)	C_{2v}	−192.15684	0.83
Li_5^+	(bipyramid)	D_{3h}	−37.38254	0.91
Na_6^+	(capped tetrahedron)	C_{2v}	−973.53324	0.68
Na_5Li^+	(capped tetrahedron)	C_s	−818.76748	0.74
$Na_4Li_2^+$	(capped tetrahedron)	C_{2v}	−664.00015	0.79
$Na_3Li_3^+$	(capped tetrahedron)	C_s	−509.22817	0.82
$Na_2Li_4^+$	(capped tetrahedron)	C_{2v}	−354.45667	0.86
$NaLi_5^+$	(capped tetrahedron)	C_s	−199.68276	0.88
Li_6^+	(capped tetrahedron)	C_{2v}	−44.90874	0.95

[a] Binding energy per atom E_b^+/n for Na_n^+ and Li_n^+: $[(n-1)E(M) + E(M^+) - E(M_n^+)]/n$, for $Na_{n-x}Li_x^+$: $[(n-x-1)E(Na) + E(Na^+) + xE(Li) - E(Na_{n-x}Li_x^+)]/n$.

[30]. Calculated adiabatic and (vertical) values are $IP(Na_2) = 4.88(4.98)$ eV, $IP(NaLi) = 4.98(5.07)$ eV, $IP(Li_2) = 5.07(5.15)$ eV. Bond lengths calculated for dimers are also in agreement. Experimental equilibrium distances are $R_e(Na_2) = 3.08$ Å [31], $R_e(NaLi) = 2.89$ Å [32], $R_e(Li_2) = 2.67$ Å [31], while calculated values are $R_e(Na_2) = 3.11$ Å, $R_e(NaLi) = 2.95$ Å, $R_e(Li_2) = 2.78$ Å.

5.2. Trimers and tetramers

Fig. 2 shows a smooth increase in the IPs as the proportion of lithium increases in triatomic clusters. Ground states of sodium and lithium trimers are obtuse isoceles. Na_2Li is obtained by substituting in Na_3 the vertex atom by a lithium atom. The optimized geometry is also an obtuse isoceles. However,

the optimized geometry for $NaLi_2$ is a triangle with a Cs symmetry and an acute angle on the sodium atom. The geometries of the neutral and cationic homogeneous and heterogeneous trimers are in close agreement with the pseudopotential CI calculations of Pavolini and Spiegelmann [27]. A comparison between experimental values and calculated values of IPs is shown in Fig. 2. The calculated IPs are globally 0.15 eV higher ($\sim 4\%$) than the experimental values. The experimental increase from Na_3 to Li_3 is well reproduced. The IPs calculated by Pavolini and Spiegelmann are in good agreement with experiment (see Table 2).

The comparison of optical absorption and ab initio calculations has allowed a precise determination of the ground state of homonuclear and heteronuclear tetramers [15,33,4,1]. Tetramers have planar rhombal structures. The most stable structures ob-
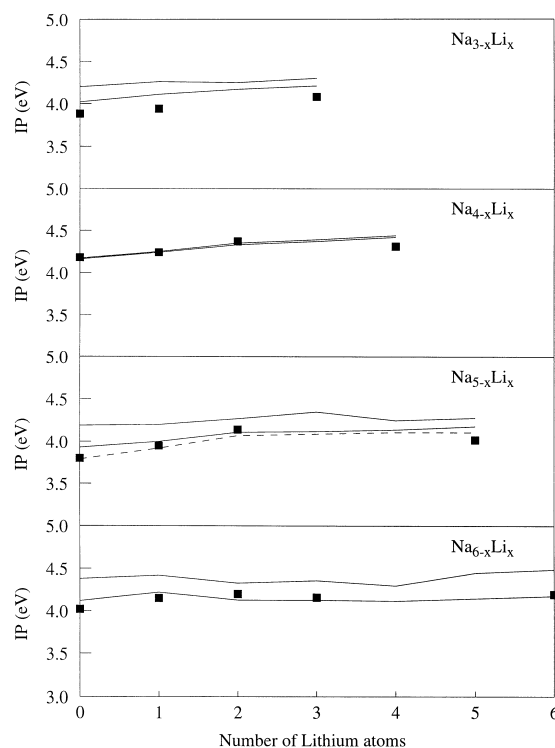

Fig. 2. Experimental IPs (squares) and calculated adiabatic (lower full line) and vertical IP (upper full line) for the lowest-energy structures plotted as a function of the number of Li atoms for sizes 3–6. For pentamers, the dashed line corresponds to the adiabatic IPs calculated for the second lowest-energy structures (see text).

tained with the present DFT/PW-91 calculations are in agreement with previous results. In mixed tetramers, lithium atoms are preferentially located on the short diagonal of the rhombus. Every cation assumes a similar rhombal structure. In particular, in contrast to results from CI calculations, we found that the T forms are less stable than the rhombal forms. This explains why the calculated vertical and adiabatic IPs are close. The agreement between the experiment and the calculation is particularly good for the IPs of tetramers (see Fig. 2 and Table 2). It is interesting to notice that the photoionization cross-sections obtained for tetramers are sharp. This is in agreement with the fact that calculated vertical and adiabatic IPs are close.

5.3. Pentamers

For pentamers and hexamers, there is a competition between planar and non-planar structures. According to previous calculations, the two most stable structures for Na_5 and Li_5 are a planar structure (symmetry C_{2v}) and a trigonal bipyramid (symmetry C_{2v}). The optical absorption of Na_5 and Li_5 have been studied, but the spectra are broad and not

precise [3,2]. They are not clearly in favor of one structure. For Na_5 the lowest-energy structure obtained from our DFT calculations is the planar structure, in agreement with previous CI calculations [21]. For Li_5 we found that the 3D structure is slighty more stable than the planar structure ($\Delta E = 0.06$ eV), while the reverse is observed from CI calculations [26]. To determine the structures of $Na_{5-x}Li_x$ clusters, we have replaced x sodium atoms by lithium atoms in all possible ways in the planar and bipyramidal structures and we have optimized each structure via gradient techniques. The most stable planar and bipyramidal structures so obtained for each cluster are shown in Fig. 3. In all these heterogeneous structures, the lithium atoms are located on the more coordinated centers. This is easily explained by the fact that the Li–Li bond or Li–Na bond are shorter and stronger than the Na–Na bond ($R_e(Li_2) < R_e(NaLi) < R_e(Na_2)$ and $D_e(Li_2) > D_e(NaLi) > D_e(Na_2)$). Then the configurations in which the number of Li–Li and Na–Li bonds is a maximum are the most stable. In sodium-rich clusters, lithium atoms induce a contraction of the lengths, which slightly deforms the structures. In lithium-rich clusters, sodium atoms tend to be on the outside of the
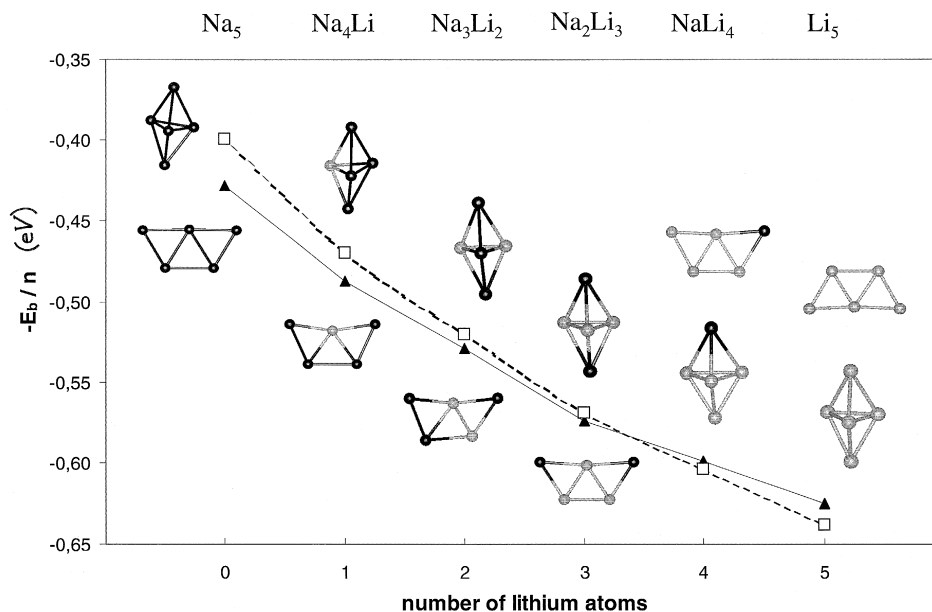

Fig. 3. Binding energies per atom $-E_b/5$ in the planar structures (triangles) and trigonal bipyramid structures (squares) of $Na_{5-m}Li_m$ clusters. The corresponding geometries are drawn.

structure so that the Li–Na distances can be relatively large while the Li–Li distances remain short. In particular, the planar structures of Na_nLi_m are obtained from the lowest-energy structure of $Na_{n-1}Li_m$ by adding 1 sodium atom on a bridge with 2 atoms. The ground states of the planar and of the bipyramidal structures are almost degenerate for every heteronuclear pentamer (the energy differences are close to the precision of the calculation). However, the comparison of the binding energies per atom $E_b/(n+m)$ for both structures shows that the stability of the non-planar structure tends to increase regularly as the number of lithium atoms increases.

For cationic clusters (see Table 3), the most stable structure that we have obtained for Na_5^+ is the two twisted triangle (or diabolo structure) as recently probed by optical absorption [5,34] and for Li_5^+ the trigonal bipyramid (D_{3h}). Na_4Li^+ and $Na_3Li_2^+$ have structures similar to Na_5^+ (with a lithium atom in the middle), $Na_2Li_3^+$ and $NaLi_4^+$ have structures similar to the best neutral structures.

The calculated IPs for the lowest-energy structures are given in Table 2 and shown in Fig. 2 There is a fair agreement with the experiment. The dashed line shows the adiabatic IP calculated for the second

structure (the less stable one shown in Fig. 3). The stabilities of the two structures are so close that it is clear that IP measurements do not allow the determination of which structure is experimentally observed. A coexistence of the two structures in the beam is not excluded. Such a coexistence was in fact suggested by the optical spectrum of Li_5 [3]. While we cannot conclude formally, the good agreement of the dashed line with the experiment may be in favor of a coexistence of structures.

5.4. Hexamers

Optical absorption of Na_6 and Li_6 have been compared to the transitions calculated for three different structures: a planar D_{3h} structure, a quasi-planar pentagonal pyramid (C_{5v}) and a tetrahedral structure (C_{2v}). For Li_6, the experimental spectrum is in good agreement with the spectrum calculated for the tridimensional C_{2v} structure while the planar and pentagonal structures can be excluded [10]. As this has been already observed from DFT calculations [35], we found that the energy of the tetrahedral structure (C_{2v}) is not a true minimum on the energy surface, it relaxes toward the more symmetrical
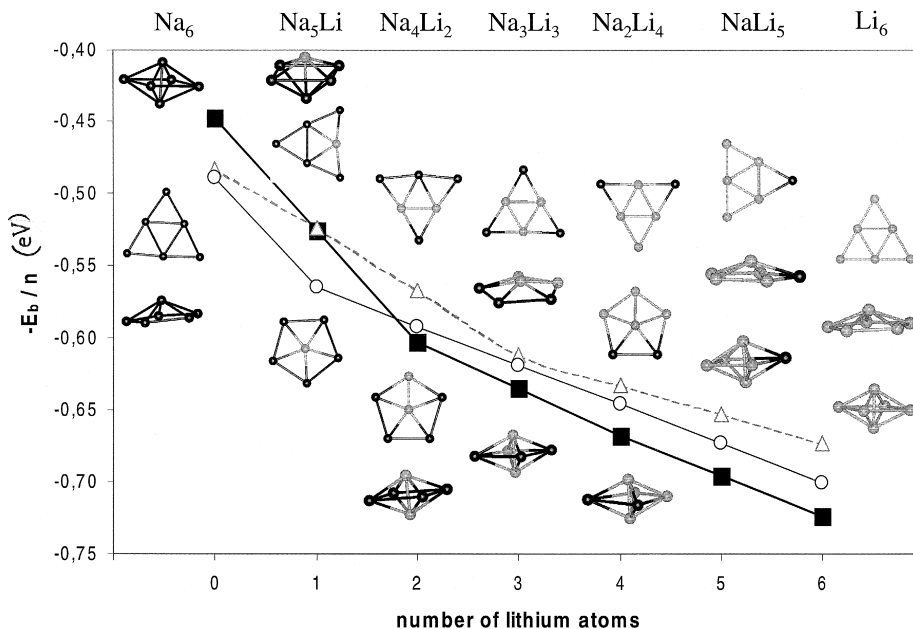

Fig. 4. Binding energies per atom $-E_b/6$ in the planar structures (triangles), pentagonal structures (circles) and bipyramid structures (squares) of $Na_{6-m}Li_m$ clusters. The corresponding geometries are drawn.

square bipyramid (D_{4h}). In contrast, for Na_6, the tridimensional C_{2v} structure can be excluded and the optical spectra are in agreement with spectra calculated for the planar and pentagonal geometries [2,4,5]. In agreement with previous optimizations, we found that these two structures are the more stable ones for Na_6. They are almost degenerate. For heterogeneous clusters, geometry optimization has been carried out for the planar, pentagonal pyramid and square bipyramid structures. Geometries have been optimized without symmetry constraint (except for the planar structure which has been optimized in 2D) and every possible permutation of atoms has been considered. Most stable geometries for every family of structures are shown in Fig. 4. The analysis of the structures obtained for mixed clusters shows that, as already observed for pentamers, lithium atoms are located on the more coordinated centers. Comparison of the binding energies per atom calculated for the different structures shows that the stability of the bipyramid structure increases as the number of lithium atoms increases (see Fig. 4). For clusters which contain at least 2 lithium atoms, the 3D bipyramid is the lowest-energy structure. We found that planar structures are clearly less stable in lithium-rich clusters than in sodium-rich clusters. In Na_6 the energy difference between the planar structure (D_{3h}) and the bipyramid (D_{4h}) is $\Delta E = 0.21$ eV in favor of the planar structure, while for Li_6 the energy difference $\Delta E = 0.31$ eV is in favor of the bipyramid. The lowest-energy structures obtained in the present work for cationic structures (see Table 3) are all constructed from the C_{2v} tetrahedral structure [5].

Fig. 2 shows that the calculated IPs for the most stable structures are close to the experimental values. The adiabatic IPs calculated for the three structures (planar, pentagonal and bipyramid) are plotted in Fig. 5 as a function of the number of lithium atoms. They are compared to experimental values. IPs obtained for the planar and quasi-planar pentagonal structures tend to decrease as the number of Li atom increases in the cluster, while the experimental values show a small increase. However, the increase observed for the bipyramid (0.30 eV) is stronger than the experimental increase (0.17 eV). In fact, for each cluster, the best agreement is obtained for the most stable calculated structure. The comparison between
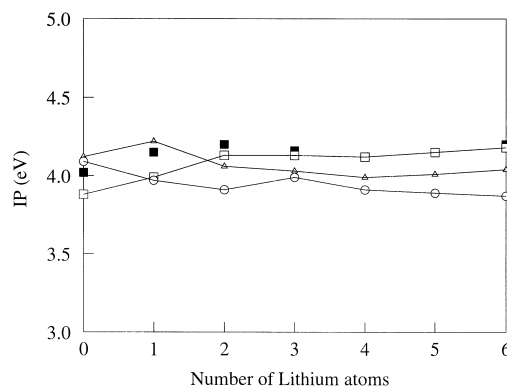
Fig. 5. Calculated adiabatic IPs for the three different structures of $Na_{6-m}Li_m$ clusters and experimental IPs (black squares) plotted as a function of the number of Li atoms. The empty squares correspond to the bipyramids, the circles to the planar structures and the triangles to the pentagonal structures.

experimental IPs and our DFT calculations is clearly in favor of a planar or quasi-planar to tridimensional transition as the number of lithium atoms increases in the cluster.

6. Conclusion

We have measured ionization potentials of mixed Na_nLi_m clusters with ($3 \leqslant n \leqslant 21$ and $1 \leqslant m \leqslant 3$) generated in a supersonic beam. For clusters containing 2–6 atoms, we have compared experimental values to the results of density functional theory calculations. Experimental values are in good agreement with the calculated values corresponding to the lowest-energy isomers. Results for sizes 5 and 6 for which the 2D–3D transition occurs in pure alkali clusters are particularly interesting. For pentamers, our calculations point to a transition from planar to tridimensional structures as the number of lithium atoms increases in the cluster. Differences in calculated energies between these two structures are too small to conclude, even if our experimental results suggest the coexistence of different isomers in the beam. For hexamers, calculated results display the same transition. For this size, the comparison experiment/theory confirms the existence of such a transition. This is in agreement with the optical spectra that were measured on Na_6 and Li_6. Finally, the analysis of the most stable structures that we have

obtained for mixed clusters shows that, in a heteronuclear cluster, the coordination of lithium atoms is superior to the coordination of sodium atoms.

References

[1] J. Blanc, V. Bonacic-Koutecky, M. Broyer, J. Chevaleyre, Ph. Dugourd, J. Koutecky, C. Scheuch, J.P. Wolf, L. Wöste, J. Chem. Phys. 96 (1992) 1793.

[2] C.R.C. Wang, S. Pollack, T.A. Dahlseid, G.M. Koretsky, M.M. Kappes, J. Chem. Phys. 96 (1992) 7931.

[3] M. Broyer, Ph. Dugourd, Comments At. Mol. Phys. 31 (1995) 183.

[4] V. Bonacic-Koutecky, P. Fantucci, J. Koutecky, Chem. Rev. 91 (1991) 1035.

[5] V. Bonacic-Koutecky, C. Fuchs, J. Pittner, L. Cespiva, P. Fantucci, J. Koutecky, Comments At. Mol. Phys. 31 (1995) 233.

[6] K. Selby, M. Vollmer, J. Masui, V. Kresin, W.A. de Heer, W.D. Knight, Phys. Rev. B 40 (1989) 5417.

[7] S. Pollack, C.R.C. Wang, M.M. Kappes, J. Chem. Phys. 94 (1991) 2496.

[8] S.A. Blundell, C. Guet, Z. Phys. D 33 (1995) 153.

[9] E. Benichou, R. Antoine, D. Rayane, B. Vezin, F.W. Dalby, Ph. Dugourd, M. Broyer, C. Ristori, F. Chandezon, B.A. Huber, J.C. Rocco, C. Guet, to be published.

[10] Ph. Dugourd, J. Blanc, V. Bonacic-Koutecky, M. Broyer, J. Chevaleyre, J. Koutecky, J. Pittner, J.P. Wolf, L. Wöste, Phys. Rev. Lett. 67 (1991) 2638.

[11] W.A. de Heer, Rev. Mod. Phys. 65 (1993) 611.

[12] I. Boustani, W. Pewestorf, P. Fantucci, V. Bonacic-Koutecky, J. Koutecky, Phys. Rev. B 35 (1987) 9437.

[13] C. Yannouleas, U. Landman, J. Chem. Phys. 107 (1997) 1032.

[14] M.M. Kappes, M. Schär, E. Schumacher, J. Phys. Chem. 91 (1987) 658.

[15] S. Pollack, C.R.C. Wang, T.A. Dahlseid, M.M. Kappes, J. Chem. Phys. 96 (1992) 4918.

[16] Ph. Dugourd, D. Rayane, P. Labastie, B. Vezin, J. Chevaleyre, M. Broyer, Chem. Phys. Lett. 197 (1992) 433.

[17] Ph. Dugourd, D. Rayane, R. Antoine, M. Broyer, Chem. Phys. 218 (1997) 163.

[18] M.L. Homer, J.L. Persson, E.C. Honea, R.L. Whetten, Z. Phys. D 22 (1991) 441.

[19] J.P. Perdew, Y. Wang, Phys. Rev. B 45 (1992) 13244.

[20] M.J. Frisch, G.W. Trucks, H.B. Schlegel, P.M.W. Gill, B.G. Johnson, M.A. Robb, J.R. Cheeseman, T. Keith, G.A. Petersson, J.A. Montgomery, K. Raghavachari, M.A. Al-Laham, V.G. Zakrzewski, J.V. Ortiz, J.B. Foresman, C.Y. Peng, P.Y. Ayala, W. Chen, M.W. Wong, J.L. Andres, E.S. Replogle, R. Gomperts, R.L. Martin, D.J. Fox, J.S. Binkley, D.J. DeFrees, J. Baker, J.P. Stewart, M. Head-Gordon, C. Gonzalez, J.A. Pople, GAUSSIAN 94, Revision B.3, Gaussian, Pittsburgh, PA, 1995.

[21] V. Bonacic-Koutecky, I. Boustani, M. Guest, J. Koutecky, J. Chem. Phys. 89 (1988) 4861.

[22] V. Bonacic-Koutecky, P. Fantucci, J. Koutecky, Phys. Rev. B 37 (1988) 4369.

[23] D.R. Lide, Handbook of Chemistry and Physics, 73rd edn. (CRC Press, Boca Raton, FL, 1992).

[24] A. Herrmann, E. Schumacher, L. Wöste, J. Chem. Phys. 68 (1978) 2327.

[25] C. Bréchignac, Ph. Cahuzac, Z. Phys. D 3 (1986) 121.

[26] V. Bonacic-Koutecky, J. Gaus, M.F. Guest, L. Cespiva, J. Koutecky, Chem. Phys. Lett. 206 (1993) 528.

[27] D. Pavolini, F. Spiegelmann, J. Chem. Phys. 87 (1987) 2854.

[28] S. Martin, J. Chevaleyre, S. Valignat, J.P. Perrot, M. Broyer, B. Cabaud, A. Hoareau, Chem. Phys. Lett. 87 (1982) 235.

[29] K.F. Zmbov, C.H. Wu, H.R. Ihle, J. Chem. Phys. 67 (1977) 4603.

[30] M. Schwarz, R. Duchowicz, W. Demtröder, Ch. Jungen, J. Chem. Phys. 89 (1988) 5460.

[31] K.P. Huber, G. Herzberg, Molecular Spectra and Molecular Structure, Constants of Diatomic Molecules (Van Nostrand Reinhold, New York, NY, 1979).

[32] F. Engelke, G. Ennen, K.H. Meiwes, Chem. Phys. 66 (1982) 391.

[33] T.A. Dahlseid, M.M. Kappes, J.A. Pople, M.A. Ratner, J. Chem. Phys. 96 (1992) 4924.

[34] C. Ellert, M. Schmidt, C. Schmitt, T. Reiners, H. Haberland, Phys. Rev. Lett. 75 (1995) 1731.

[35] R.O. Jones, A.I. Lichtenstein, J. Hutter, J. Chem. Phys. 106 (1997) 4566.